VAWT support structure mass sensitivity due to aerodynamic load scaling

VAWT support structure mass sensitivity due to aerodynamic load scaling

Adriana Correia da Silva, Michael Muskulus
Norwegian University of Science and Technology NTNU, Trondheim, Norway
E-mail: adriana.c.d.silva@ntnu.no

Abstract.
The X-rotor wind turbine is an X-shaped hybrid vertical axis wind turbine whose power take-off is done by horizontal axis rotors located at the tip of the lower blades. Based on an initial basic study, the present study developed a preliminary jacket design as the turbine support structure. Steady aerodynamic loads were obtained from an actuator cylinder model and dynamic load simulations including wave loads were performed. The structure was checked according to fatigue damage and maximum yielding for representative site-specific load cases for fatigue and ultimate limit states. Even though the use of a conventional jacket was shown to be feasible for the new turbine concept, the overall mass of the support structure obtained by the higher fidelity model was higher than the initial prediction. The design was driven by the fatigue damage, caused by large cyclical loads on every rotor rotation. The effect of a hypothetical aerodynamic load reduction on the jacket mass was investigated. The developed design methodology was also applied to the design of equivalent jackets after a load reduction of 75% and 50% and the mass of the structure was shown to be sensible, with a respective reduction of 25% and 48%. This result demonstrates that different design strategies that influence the magnitude of the aerodynamic loads (e.g. the control strategy) could lead to a more cost-efficient jacket design.

1. Introduction

The urge for energy cost reduction encourages the development of disruptive technologies. The X-Rotor wind turbine, illustrated in Figure 1, is a new hybrid vertical axis wind turbine (VAWT) [1] with main mechanical components (e.g. drivetrain, bearings, and secondary rotors - responsible for the power take-off) located at lower heights. Thus, the demand for heavy-lift vessels is reduced, consequently reducing installation and maintenance costs in offshore sites. Besides, constant gravitational loads may also become an advantage in comparison with ultra-large HAWTs, whose cyclical loads due to the weight of the blades becomes relevant for the fatigue design.

As larger offshore VAWT technology matures, it is expected that the shallow offshore sites near the coast get occupied, leaving to new projects intermediate to deep waters. Thus, to avoid inherit challenges of a floating platform in addition to the initial understanding of the X-Rotor wind turbine, it was decided that a jacket will be adopted as a support structure on this project, as it is more suitable to intermediate waters than monopiles. These frame structures are typically used in intermediate water depths by the wind industry and are composed of legs and brace elements that are welded together. However, VAWTs in general generate high cyclical loads that challenge the structural design in terms of the fatigue of its elements.

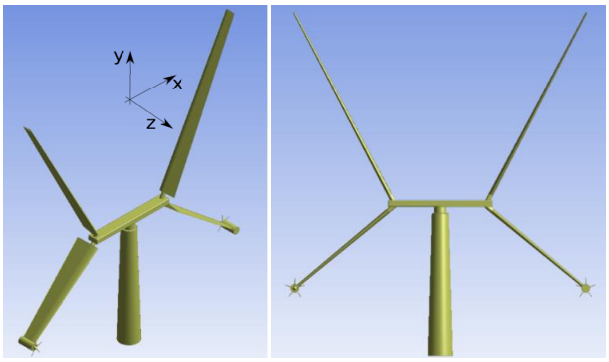

Figure 1. Representation of X-Rotor wind turbine concept and adopted coordinate system that represents the rotor at azimuth position $\phi = 0$ rad. Adapted from [1].

The present study suggests a design methodology and demonstrates a feasible preliminary design of the 2-bladed X-Rotor wind turbine jacket. The effect of a hypothetical aerodynamic load reduction is investigated by comparing the final mass of equivalent designs obtained by the proposed design methodology.

2. Design methodology

In order to simulate the performance of the X-Rotor wind turbine support structure, environmental loads and structural model are described in this section. The design assessment was based on the methodology suggested by the DNV standards [2, 3, 4].

2.1. Environmental Loads

The data from a representative site at the North Sea Center [5] with 40 m of water depth was used to design the support structure.

The aerodynamic loads were obtained for forty five rotor azimuth positions by actuator cylinder theory, which returns the mean wind loads per blade unit length. Turbulence was not considered The blade span-wise steady aerodynamic loads were provided by [6] in terms of airfoil normal and tangential forces, as well as pitching moment, under the assumption of a rigid two-bladed rotor. These components were geometrically combined to obtain the resultant forces and overturning moments that were applied at the tower top.

The wave forces were calculated using the Morison formulation and took into consideration irregular sea states with JONSWAP wave spectrum. Marine growth was considered from the sea bottom to two meters below the mean sea water line with density and thickness of 1325 kg/m and 60 mm, respectively. No current was considered.

2.1.1. Design Load cases The support structure needs to safely withstand the environmental loads to which it is subjected during the design life time. Thus, to represent these conditions, the fatigue and extreme load cases are described.

To reproduce the operational conditions over the turbine lifetime, the design situation 1.2 from [3] was defined by lumping the long-term environmental conditions described by the wind and wave joint probability distributions of the North Sea Center site [5]. The significant wave height (H_s), peak period (T_P), corresponding probabilities (p) of different sea states and rotor rotational speed (ω_r) are described in Table 1. Eighteen load cases cover the power production of the turbine. The table also shows the fixed angle, (θ) which the upper blades are pitched on each wind speed.

To illustrate the load magnitude, the resulting lateral loads applied at the tower top are shown in Figure 2 over the rotor azimuth positions, where Fz and Mz are the force and overturning moment in the direction of the wind and Fx and Mx the respective force and moment in the direction parallel to the wind.

In order to perform the dynamic simulations, these loads were converted to time series assuming the constant rotational speeds (ω_r), provided by [6] and shown in Table 1. $12.5m/s$ marks the rated wind speed, [1].

The secondary rotors located at the tip of the lower blades produce a thrust force that is assumed to balance the tower top torsional component of the aerodynamic loads, M_y, during normal operation. Thus, M_y was not included on the fatigue analysis.

Table 1. Lumped fatigue load cases used for fatigue damage estimation

LC	$U_{10}(m/s)$	$H_s(m)$	$T_P(s)$	p	$\omega_r(RPM)$	$\theta(deg)$	LC	$U_{10}(m/s)$	$H_s(m)$	$T_P(s)$	p	$\omega_r(RPM)$	$\theta(deg)$
1	<3.5	-	-	0.084	2.22	0	10	12.0	2.4	7.3	0.063	7.64	4
2	4.0	0.9	7.6	0.063	2.55	4	11	13.0	2.6	7.4	0.051	7.96	-9.7
3	5.0	1.0	7.5	0.077	3.18	4	12	14.0	2.9	7.5	0.040	7.96	-14.2
4	6.0	1.2	7.4	0.088	3.82	4	13	15.0	3.2	7.5	0.030	7.96	-14.7
5	7.0	1.4	7.3	0.094	4.46	4	14	16.0	3.4	7.6	0.021	7.96	-15.2
6	8.0	1.5	7.3	0.095	5.28	4	15	17.0	3.7	7.7	0.015	7.96	-15.9
7	9.0	1.7	7.3	0.092	5.73	4	16	18.0	4.0	7.9	0.010	7.96	-16.7
8	10.0	2.0	7.3	0.084	6.37	4	17	19.0	4.3	8.0	0.006	7.96	-17.6
9	11.0	2.2	7.3	0.074	7.00	4	18	> 19.5	-	-	0.006	7.96	-18.1

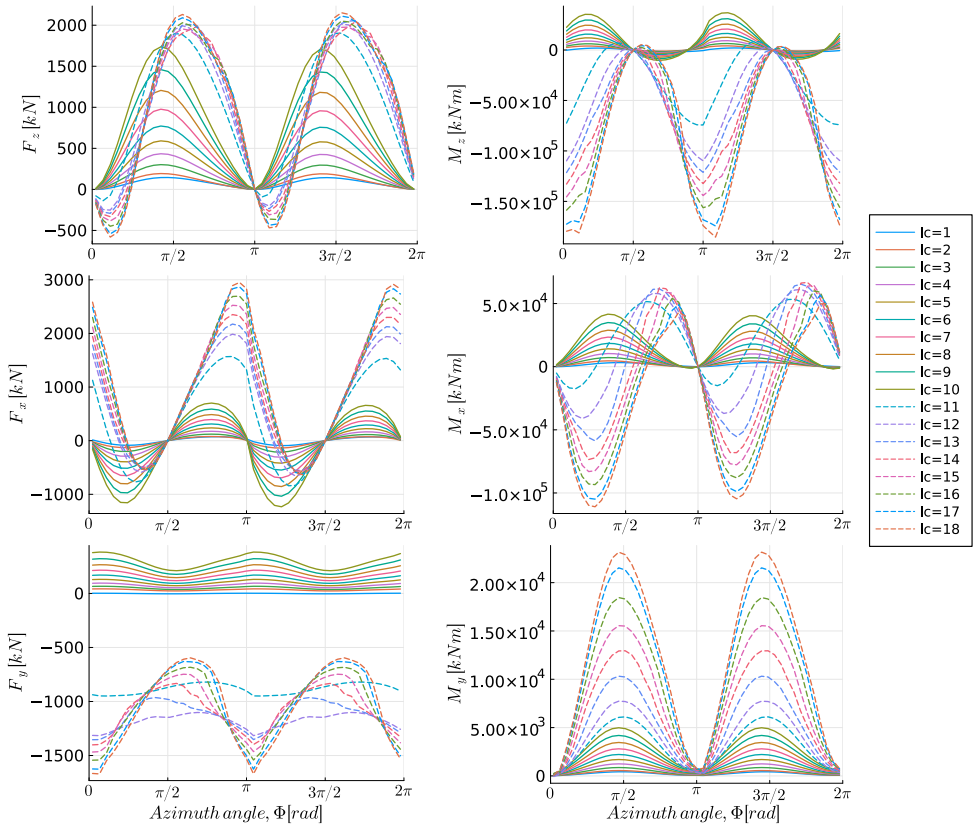

Figure 2. Operational aerodynamic loads used for fatigue damage assessment. Adapted from [6].

An extreme event with 50 year return period was considered to assess the yielding limit of the structure. A wind speed of 36.5 m/s at 70 m above the mean sea level was assumed, together

with an extreme wave with a significant wave height of $H_{s,50} = 10.1\,\mathrm{m}$ and conditional peak period of $T_p = 14.1\,\mathrm{s}$.

The resultant aerodynamic forces and overturning moments components are applied quasi-statically at the tower top (Figure 3).

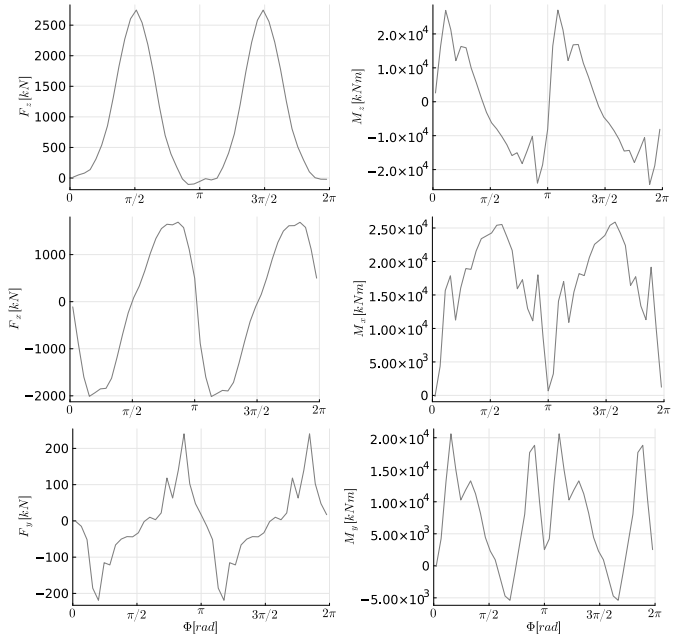

Figure 3. Extreme aerodynamic loads for $U_{70} = 36.5\,\mathrm{m/s}$ when upper blades are in flag position ($\theta = 0\,\mathrm{deg}$). Adapted from [6].

2.2. Structural Model

The Upwind four-legged jacket was used as reference [7]. This jacket was designed for the NREL 5 MW baseline horizontal axis wind turbine [8] that has slightly less rated power than the 5.5 MW estimate for X-Rotor wind turbine in its initial study [1].

VAWTs generally generate relatively larger lateral aerodynamic loads in comparison with standard HAWTs. To account for this difference and balance the resulting overturning moments, the top and bottom widths of the UpWind reference jacket were enlarged by a factor of 2.5 in the first design assessment made by [9]. These dimensions were fixed as 20 m and 30 m, respectively, for the X-Rotor jacket in this study.

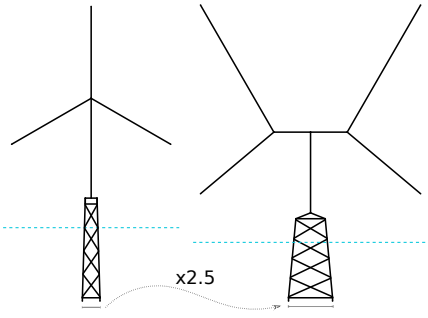

Figure 4. Upscaling of the Upwind jacket (left) bottom and top widths by a factor of 2.5 to improve overturning capacity of X-Rotor jacket (right).

For simplicity, the basic model used in this study has elements with constant cross-sections throughout the brace and legs members. Thus, from the sea bed to the jacket top, all the braces have the same diameter and thickness. The same is valid for the legs. The joint classification should be done based on the joint geometry and loading distribution within the members at each time step. However, the conservative classification recommended by [4] is adopted and Y joints are assumed on the brace connections to the legs, while X-joints are adopted for the inter-connections between braces.

The simulations were performed by FEDEM WindPower (v.7.2.1), which is a flexible multi-body solver designed for time-domain simulations. Beam elements based on Euler-Bernoulli theory were used to model the legs and brace elements.

A stiffness proportional damping coefficient of 1% was adopted and no aerodynamic damping was considered in this study. The soil-structure interaction was disregarded and the jacket legs clamped at the sea bed. The aerodynamic loads are applied at the top of a $55m$ tower composed of 4 sections designed by a quasi-static analysis for fatigue damage and yielding stress. The tower is connected to the jacket by a transition piece modelled with rigid beams whose mass of 473 tonnes was maintained from the initial basic design [9]. The rotor equivalent mass was included as a point mass at the tower top and the mass estimatied for bearings and shaft, as well as for miscellaneous electrical components (e.g. power transformer and cables), were lumped on their estimated positions along the tower nodes.

2.3. Structural analysis

The response time series obtained were post-processed by an in-house code check developed to assess the design limits in terms of fatigue and ultimate limit states.

Nominal stresses were calculated by superposing the contributions from the in-plane (M_{IP}) and out-of-plane moments (M_{OP}) with the one from the axial force (N) for the braces. The stress concentration factors (SCF) follow the Efthymiou formulation, including thickness correction. The eight hot spot stresses (HSS) on the weld connection of each brace element on the jacket tubular joints, Figure 5, were defined following the recommendations of DNV-RP-C203 [4].

The large lateral loads from the rotor require a large overturning capacity, which causes significant dynamic stresses in the axial direction of the legs. Therefore, the further recommendation from [4] was considered and the stresses from the leg elements were multiplied by a factor of 1.2 (to account for the geometrical effects on the brace connection) and combined with the stresses on the equivalent crown toe and crown heel brace´s hot spots, HSS_1 and HSS_5, respectively, as demonstrates Equations 1.

$$
\begin{aligned}
HSS_1 &= SCF_{AC}\,\sigma_x + SCF_{MIP}\,\sigma_{my} + 1.2\,\sigma_{leg} \\
HSS_2 &= \frac{1}{2}(SCF_{AC} + SCF_{AS})\,\sigma_x + \frac{1}{2}\sqrt{2}\,SCF_{MIP}\,\sigma_{my} - \frac{1}{2}\sqrt{2}\,SCF_{MOP}\,\sigma_{mz} \\
HSS_3 &= SCF_{AC}\,\sigma_x - SCF_{MOP}\,\sigma_{mz} \\
HSS_4 &= \frac{1}{2}(SCF_{AC} + SCF_{AS})\,\sigma_x - \frac{1}{2}\sqrt{2}\,SCF_{MIP}\,\sigma_{my} - \frac{1}{2}\sqrt{2}\,SCF_{MOP}\,\sigma_{mz} \\
HSS_5 &= SCF_{AC}\,\sigma_x - SCF_{MIP}\,\sigma_{my} + 1.2\,\sigma_{leg} \\
HSS_6 &= \frac{1}{2}(SCF_{AC} + SCF_{AS})\,\sigma_x - \frac{1}{2}\sqrt{2}\,SCF_{MIP}\,\sigma_{my} + \frac{1}{2}\sqrt{2}\,SCF_{MOP}\,\sigma_{mz} \\
HSS_7 &= SCF_{AC}\,\sigma_x + SCF_{MOP}\,\sigma_{mz} \\
HSS_8 &= \frac{1}{2}(SCF_{AC} + SCF_{AS})\,\sigma_x + \frac{1}{2}\sqrt{2}\,SCF_{MIP}\,\sigma_{my} + \frac{1}{2}\sqrt{2}\,SCF_{MOP}\,\sigma_{mz}
\end{aligned}
\tag{1}
$$

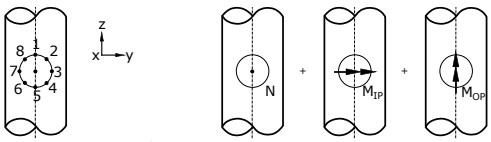

Figure 5. Superposition of stresses for tubular joints on 8 hot spot points. Adapted from [4].

This study focused on the assessment of fatigue damage and ultimate stresses under extreme conditions. Thus, both fatigue limit states (FLS) and ultimate limit states (ULS) were evaluated as follow:

The Palmgren-Miner rule was used to evaluate the accumulated damage and the rainflow method adopted to count the number of times, n_i, a stress range, $\Delta\sigma_i$, occurs in the signal. The total damage D is calculated

by multiplying the accumulated damage with its probability of occurrence p_i, as shown in Equation 2.

$$D = \sum_i \frac{n_i}{N_i} p_i \tag{2}$$

The S-N curves for tubular joints were adopted from DNV-RP-C203 [4] for above and below the mean sea water line as "in air" and "in sea water with cathodic protection", respectively. The total damage was scaled to the design life time of 20 years and no inspections were assumed to occur during this period. Thus, the damage was multiplied by a design fatigue factor (DFF) of 3, as per the standard.

The ultimate yielding strength of the design was checked by evaluating the maximum absolute value of the hot spot stresses σ_{1-8} for the extreme event of 50 year return period. Material and load safety factors of 1.1 and 1.25 were applied, respectively.

2.4. Design Strategy

An initial basic design of the X-rotor jacket [9] was obtained by an estimation of the stress ranges through a quasi-static analysis, where 20% of the fatigue damage utilization was reserved for hydrodynamic effects - not included in the initial model. Here, the same safety margin of 20% is adopted to account for dynamic effects not included in the model, such as aerodynamic damping, turbulence and fluctuations of the secondary rotors thrust. From these initial dimensions, the present study aimed to obtain a feasible design when including hydrodynamic effects and joint detailing considerations in terms of SCFs in a dynamic analysis.

The strategy adopted consisted of an attempt to increase the stress bearing capacity of the members' cross-sections by enlarging their dimensions. In order to reduce the number of design parameters, the value of brace diameter d_b, brace thickness t_b, as well as leg thickness t_l were linked to the leg diameter d_l, which was increased until the safety requirements were reached.

In parallel, an attempt to reduce the SCFs was made, as these values also influence the final stresses, which can be seen in Equation 1. This was done by reducing the legs' radius-to-thickness $\gamma = d/2t$ to a value of 8, the minimum value that still respects the validity of the Efthymiou formulation. Figure 6 illustrates the tendency of SCF reduction for a lower γ value. However, τ was fixed to a similar value as used on the Upwind jacket with the aim to maintain the relative stiffness between legs and braces.

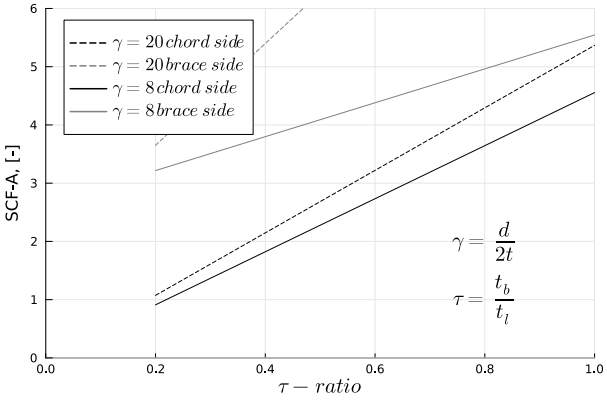

Figure 6. Effect of γ-ratio and τ-ratio on the chord side SCF and brace side SCF in a Y joint. Adapted from [10]

Later, the design methodology was repeated to obtain equivalent jacket designs for the cases when the aerodynamic loads were scaled down, whose final mass comparison is the goal of this study.

3. Results and discussion

3.1. Preliminary design

Similarly to the case of HAWTs, it was observed that fatigue drives the sizing of the elements of X-Rotor jacket. The high cyclical operational loading, as illustrated in Figures 7 and 12, for the most critical HSS_5, leads to a jacket of 2984 tons. The dimensions of legs and brace elements are shown in Table 2.

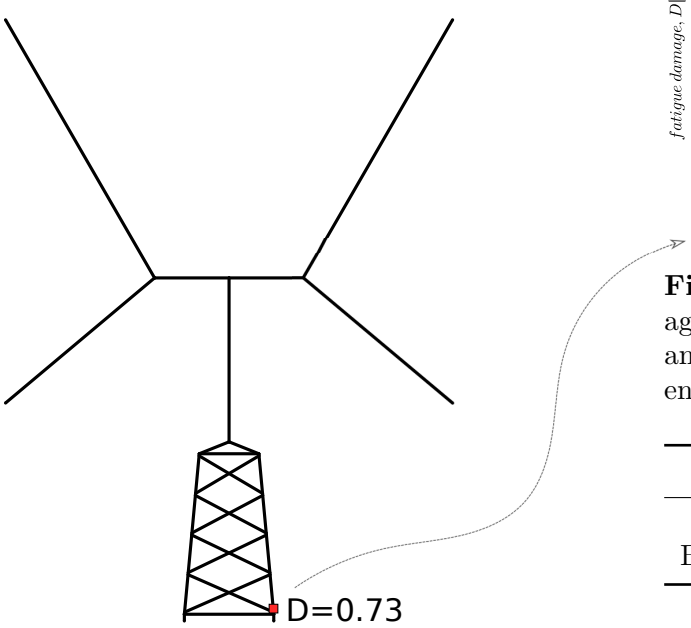

Figure 7. Maximum damage D at the critical hot spot (indicated by a red square).

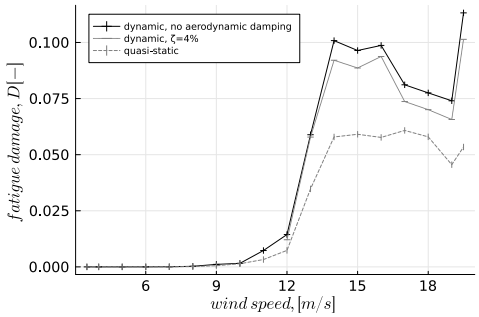

Figure 8. Comparison between damages from quasi-static and dynamic analysis at the critical point for different wind speeds.

[-]	Diameter (m)	Thickness(mm)
Legs	1.835	114
Braces	1.10	68

Table 2. X-Rotor jacket members dimensions for the the baseline design.

It is observed that most damage occurs for the load cases above rated wind speed, as shown in Figure 8, when the upper blades start to negatively pitch (Table 1) in order to control the power production of the turbine. This increase of the damage is expected, as the magnitude of the loads are enlarged on this range (Figure 2), showing how sensitive the aerodynamic loads are to the adopted control strategy. This hints at the possibility of potentially reducing the loads (with small losses in production) through a more tailored control strategy.

Figure 8 also demonstrates an influence of dynamic effects by comparing the damage on the most critical point when a quasi-static and dynamic analyses are performed. Due to the 2-bladed rotor configuration, Figure 1, most of the frequency content of the aerodynamic loads applied at the tower top is located at the 2 P and 4 P frequencies. However, some higher harmonics from the aerodynamic loads, visible in the M_z amplitude spectrum, Figure 9, can potentially excite the structure if coinciding with its first natural frequency f_1. Therefore, the increase of cross-section parameters resulted in a stiff jacket whose natural frequency, $f_1 = 1.66$ Hz, avoided these harmonics, as observed in Figure 10.

Despite the dynamic effect from higher load harmonics, the aerodynamic damping is shown to have a low influence on the final damage, as demonstrated in Figure 8 for the wind speeds above rated when a hypothetical aerodynamic damping ratio, ζ, of 4 % was considered. Even though the effects of turbulence can be considerable on the fatigue damage assessment of jacket support structures of horizontal axis wind turbines, the X-Rotor wind turbine concept generates high load cycles from the mean wind, and the effects from the turbulence are also considered to

be negligible to the fatigue damage.

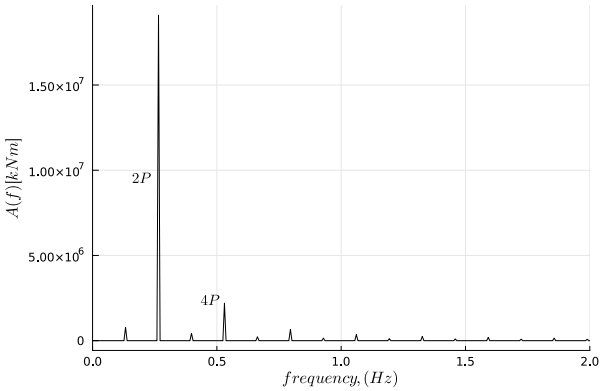

Figure 9. Amplitude spectrum of the aerodynamic overturning moment in the wind direction M_z for $lc = 11$ ($U = 13m/s$) applied at the tower top.

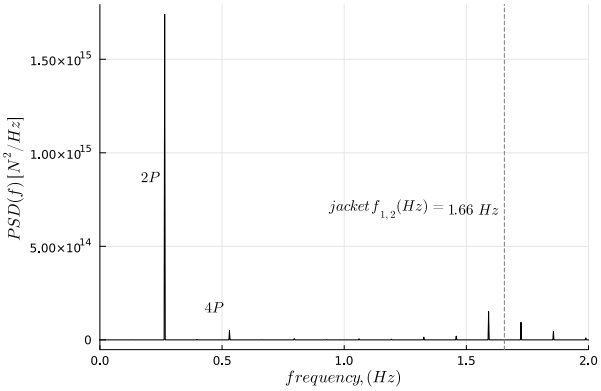

Figure 10. Power density spectrum (PSD) of the axial force from the leg in the critical hot spot, when no waves are applied, for $lc = 11$ ($U = 13\,\mathrm{m/s}$).

The aerodynamic load components corresponding to an extreme event of 50 year return period were statically applied to the tower top under the assumption that the turbine is parked. The response was linearly combined with the one from an extreme sea state of 50 year return period. This resulted in a maximum stress of $\sigma = 192.9\,\mathrm{MPa}$ on one of the jacket bottom connections.

3.2. Load Reduction

Although a feasible jacket design has been obtained, it is still relatively heavy in comparison with substructures of equivalent rated-power wind turbines.

As a new concept, the X-Rotor wind turbine still possesses design space to reduce the aerodynamic loads by changing the control strategy. Therefore, in order to better understand the effect such a load reduction has on the jacket support structure, the aerodynamic loads were scaled down, and new designs with similar fatigue utilization ratios were obtained for comparison. Figure 11 shows the resultant jacket mass versus the percentage by which the aerodynamic loads were scaled down. A significant mass reduction of 25% and 48% is observed for a reduction of 75% and 50% in loads, respectively.

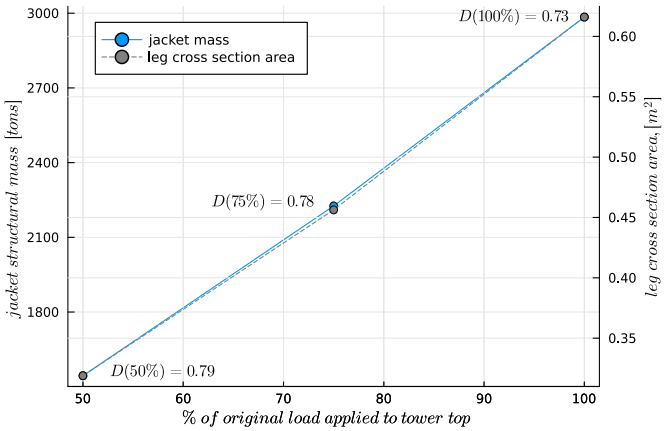

Figure 11. Jacket mass and respective leg cross-section area with respect to aerodynamic load reduction. The equivalent fatigue utilization ratio for each feasible design at the critical point is denoted by D.

Interestingly, the load reduction seems to have a linear effect on the jacket mass. This can be explained as follows:

(i) Only the magnitude of the aerodynamic loads is scaled down, while the number of cycles is maintained, as it is determined by a fixed rotor rotational speed.

(ii) The loading cycles on the stress response are mainly caused by the aerodynamic loads, even though the equivalent natural frequencies of the jackets slightly change, as shown in Figure 12. Therefore, the number of cycles n_i from Equation 2 is maintained.

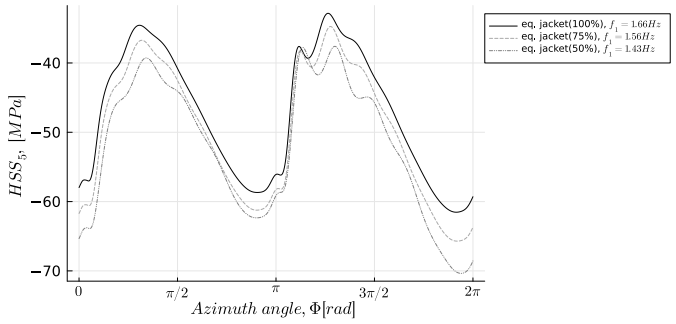

Figure 12. Comparison of a typical stress-signal from the same critical point (HSS_5) on the equivalent jacket desings after load reduction.

(iii) The critical point remains the same on the equivalent jackets. Together with consideration (i), to maintain the similar utilization ratios D, the maximum allowed number of cycles N_i of each stress range should be maintained. This is observed in Figure 12 as the stress range stays approximately equal despite the shift around the mean stress, which does not influence the damage estimated from an S-N curve.

(iv) Most part of the stress ranges on the critical point (HSS_5 of Equations 1) come from the axial force from the leg. Thus, the leg cross-section areas, which have a linear behavior within the equivalent jackets, dictate the most influence on these stress ranges. Meanwhile, the contribution from the braces, which would augment the non-linear effects due to the SCFs, are reduced. This results in a roughly linear relationship between the load reduction and the jacket mass.

4. Conclusions

This study developed a feasible preliminary design for the jacket of the X-Rotor wind turbine and demonstrated a linear reduction in its mass with respect to a hypothetical reduction of the aerodynamic loads. This information is useful in taking further design decisions in the project, e.g., with respect to possible changes in the control strategy.

It was shown that the design is driven by the fatigue limit state and that a stiff design of 1.66 Hz and 2984 tons was required to withstand the large cyclic aerodynamic loads, typical from VAWTs. It was found that these loads contain higher harmonics close to the first natural frequency of the support structure and care should be taken to avoid resonance.

As a new concept, there is still some uncertainty related to the aerodynamic damping of the X-Rotor turbine, but its effect was considered to be negligible. In addition, the effect of turbulence was not considered, as the natural frequencies of the stiff jacket designs presented (1.43 Hz, 1.56 Hz, and 1.66 Hz) are far above this excitation and only the mean wind loads obtained from an actuator cylinder model were considered. So, it is highlighted that the presented results regarding fatigue damage, and thus, the jacket design should be treated as preliminary.

It was demonstrated that most damage is generated at the higher wind speeds above rated speed, when the upper blades are negatively pitched. Different control strategies could reduce

the aerodynamic loads and, consequently, the fatigue damage. For a load reduction of 75 % and 50 %, a structural mass reduction of 25 % and 48 % was obtained, respectively.

For simplicity, the study assumed a constant cross-section for all the braces, as well as for the legs. In addition, the ratio between the diameters and thicknesses of these members was fixed, aiming for a partial reduction of the SCFs, which depends largely on this ratio.

Apart from a hypothetical load reduction, a more cost-efficient design could be obtained when these parameters are independently optimized for each location. Also, the inclusion of joint cans would allow lighter members, as the cross-sections far from the connections would not be unnecessarily large. Due to all these limitations, there is still a relatively wide margin for mass reduction and a great potential for more cost-efficient and competitive designs.

Acknowledgements

The authors acknowledge the European Union's Horizon 2020 research and innovation programme from which X-ROTOR project received funds under grant agreement No 101007135.

The authors also acknowledge Jing Dong, from the Norwegian University of Science and Technology NTNU, Abbas Kazemi Amiri, William Leithead and David Campos, from the University of Strathclyde, and Adhyanth Giri Ajay and Carlos Ferreira from Delft University of Technology for the valuable discussion and contribution with data that made this study possible.

Author Contribution Statement

ACDS developed the model in FEDEM, performed the analysis, post-processed the results, and wrote the paper. MM coordinated the study, formulated the goals, and provided expertise. All authors contributed to the design of the methodology, interpretation of the results, and review of the final manuscript.

References

[1] Leithead W, Camciuc A, Amiri A K and Carroll J 2019 *Journal of Physics: Conference Series* **1356** 012031
[2] DNV GL 2016 Support structures for wind turbines DNVGL-ST--0126
[3] DNV GL 2016 Loads and site conditions for wind turbines DNVGL-ST-0437
[4] DNV GL 2016 Fatigue design of offshore steel structures DNVGL-RP-C203
[5] Li L, Gao Z and Moan T 2015 *Journal of Offshore Mechanics and Arctic Engineering* **137**
[6] Ferreira C 2021 Aero-elastic dynamic model capable of modelling the X-Rotor Tech. Rep. WP2-D2.1 TU Delft Delft, Netherlands
[7] Vorpahl F, Popko W and Kaufer D 2013 *Description of a basic model of the "UpWind reference jacket" for code comparison in the OC4 project under IEA wind annex 30* URL `https://publica.fraunhofer.de/handle/publica/296668`
[8] Jonkman J, Butterfield S, Musial W and Scott G 2009 Definition of a 5-MW Reference Wind Turbine for Offshore System Development Tech. Rep. Technical Report NREL/TP-500-38060 National Renewable Energy Laboratory (NREL) United States
[9] Amiri A K 2021 X-Rotor, an innovative offshore wind turbine. Background and draft design configurations Tech. Rep. v1 University of Strathclyde Glasgow, UK
[10] Lotsberg I 2016 *Fatigue Design of Marine Structures* (Cambridge University Press)